SIN-CHN SCIENTIFIC PRESS PTE.LTD.

Molecular & Cellular Biomechanics 2025, 22(3), 1357.
https://doi.org/10.62617/mcb1357

Article

Zanthoxylum bungeanum-derived extracellular vesicles alleviate liver fibrosis via TGF-β1/Smad pathway

Tao Jiang[1,2], Ruiling Fan[3], Bingqi Zhang[2], Juan Xiong[4], Ningjing Pu[5], Mingcai Zhao[6], Qianyuan Gong[2,*], Yuanbiao Guo[1,2,*]

[1] School of Laboratory Medicine, North Sichuan Medical College, Nanchong 637100, China
[2] Medical Research Center, The Affiliated Hospital of Southwest Jiaotong University, The Third People's Hospital of Chengdu, Chengdu 610031, China
[3] Institute of Materia Medica, School of Pharmacy, North Sichuan Medical College, Nanchong 637100, China
[4] Department of Laboratory Medicine, Chengdu Qingbaijiang District People's Hospital, Chengdu 610300, China
[5] Department of Laboratory Medicine, The Third People's Hospital of Chengdu, Chengdu 610031, China
[6] Department of Laboratory Medicine, Suining Central Hospital, Suining 629000, China
*** Corresponding authors:** Qianyuan Gong, gqyscu@sina.cn; Yuanbiao Guo, guoyuanbiao@swjtu.edu.cn

CITATION

Jiang T, Fan R, Zhang B, et al. *Zanthoxylum bungeanum*-derived extracellular vesicles alleviate liver fibrosis via TGF-β1/Smad pathway. Molecular & Cellular Biomechanics. 2025; 22(3): 1357. https://doi.org/10.62617/mcb1357

ARTICLE INFO

Received: 13 January 2025
Accepted: 6 February 2025
Available online: 19 February 2025

Abstract: The activation of hepatic stellate cells (aHSCs) play a role for the occurrence and progression of liver fibrosis. However, effective drugs that can prevent or reverse this pathological process remain unavailable. Zanthoxylum bungeanum Maxim. (Rutaceae) is an edible and medicinal plant with diverse bioactivities, including antiparasitic, antimicrobial, and anti-inflammatory effects. This study investigates the therapeutic potential and underlying mechanisms of Zanthoxylum bungeanum-derived extracellular vesicles (ZEVs) in liver fibrosis, using the human HSCs LX-2 cells and alcohol-induced mice model of liver fibrosis. The results show that ZEVs significantly inhibit the proliferation and migration of LX-2 cells, while downregulating the fibrosis-related proteins and genes expression. Furthermore, oral administration of ZEVs significantly decreased serum alanine aminotransferase (ALT) and aspartate aminotransferase (AST) levels in mice with liver fibrosis, reducing liver inflammation, collagen deposition, and lipid droplet accumulation. Additionally, miR-9 and miR-17 in ZEVs were found to significantly reduce the synthesis of fibrosis-related proteins in activated LX-2 cells. Mechanistic studies further revealed that ZEVs suppressed the gene levels of TGF-β1, Smad2 and Smad3 in activated LX-2 cells. In conclusion, ZEVs are a possible treatment option for liver fibrosis, potentially through modulation of the TGF-β1/Smad signaling pathway.

Keywords: alcohol; edible and medicinal plant; liver fibrosis; hepatic stellate cells

1. Introduction

Accumulation of extracellular matrix (ECM) is characteristic of hepatic fibrosis, resulting in the development of fibrous scars that alter liver structure [1]. This disruption results in hepatocyte depletion, functional impairments, and eventual liver failure [2]. Liver fibrosis can be induced by liver injuries caused by toxic, metabolic or viral factors [3]. In China, approximately 300 million people are affected by chronic liver diseases, a significant proportion of whom experience varying degrees of liver fibrosis [4].

Activated hepatic stellate cells (aHSCs) play a significant part in the pathogenesis of liver fibrosis [5]. Under normal conditions, HSCs store vitamin A of liver in quiescent state (qHSCs) [6]. Following liver injury, inflammatory signals activate qHSCs, converting them into myofibroblasts [7]. As a result, aHSCs secrete

ECM proteins and matrix metalloproteinases, driving liver tissue remodeling [8,9]. Therefore, therapeutic strategies targeting aHSCs are considered effective in slowing or potentially reversing liver fibrosis [10]. The progression of liver fibrosis is strongly linked to human HSCs LX-2. Both LX-1 and LX-2 cells express α-smooth muscle actin (α-SMA), a marker of activated HSCs [11]. *In vitro* studies have shown increased α-SMA and type I collagen (COL I) protein expression in activated LX-2 cells [12].

Extracellular vesicles (EVs), ranging in size from 40 to 100 nm, are natural nanoparticles secreted by cells [13]. Studies have demonstrated that plant-derived EVs exhibit protective effects against liver injury. For example, in mice with alcoholic liver injury, treatment with ginger-derived EVs resulted in a reduction in serum triglyceride levels, diminished liver lipid accumulation, and a decrease in liver weight [14]. EVs derived from black mulberry (*Morus nigra L.*) leaves were observed to cause cell cycle arrest at the G0/G1 phase, inhibit migration, increase intracellular reactive oxygen species (ROS) levels and ultimately promote apoptosis in Hepa1-6 liver cancer cells [15]. Additionally, EVs from *Asparagus* inhibited the proliferation of HepG2 liver cancer cells, upregulated apoptosis-related factors and induced apoptosis [16]. Furthermore, tea-derived EVs reduced COL I and α-SMA proteins expression in LX-2 cells via the TGF-β1/Smad signaling pathway [17].

Zanthoxylum bungeanum (ZB), distributing in China, Japan and Korea, contains numerous active constituents, including hydroxy-α-sanshool, hydroxy-β-sanshool, hydroxy-c-sanshool, skimmianine, nerol, α-pinene, c-sanshool, linalool, zanthobungeanine, β-sitosterol, and piperitone [18,19]. Studies have demonstrated that ZB possesses antidiabetic, antibacterial, antiparasitic, and anti-inflammatory properties [20]. Additionally, ZB extracts have been shown to exert hepatoprotective effects. ZB alleviates non-alcoholic fatty liver disease (NAFLD) in mice by modulating fatty acid and cholesterol metabolism, as well as the gut microbiota [21]. *Pericarpium Zanthoxyli* extract has been shown to ameliorate mitochondrial dysfunction in HepG2 cells and reverse the increase in H_2O_2 and decrease in glutathione, thus alleviating liver tissue damage induced by CCl_4 [18]. Researches have shown that ZB amide reduces the levels of aspartate aminotransferase (AST), alanine aminotransferase (ALT), triglycerides, total cholesterol, and the number of lipid droplets in liver tissues of NAFLD mice through the AMPK/Nrf2 signaling pathway [22]. However, the effect of *Zanthoxylum bungeanum*-derived extracellular vesicles (ZEVs) on liver fibrosis is currently unclear.

Thus, this study aims to investigate the therapeutic benefits of ZEVs in liver fibrosis and the underlying mechanisms. Our findings demonstrated that ZEVs effectively ameliorated liver fibrosis in both activated LX-2 cells and liver fibrosis mice. Additionally, we performed sequencing of 18-24 nt microRNAs (miRNAs) in ZEVs and identified that two of the most abundant miRNAs, miR-9 and miR-17, significantly reduced the levels of fibrosis-related proteins in activated LX-2 cells. Further mechanistic studies demonstrated that ZEVs inhibited the mRNA levels of TGF-β1, Smad2 and Smad3 in activated LX-2 cells. In conclusion, the results demonstrate that ZEVs hold promise as innovative therapeutic biomaterials for liver fibrosis.

2. Methods

2.1. Separation and purification of ZEVs

ZB samples were obtained from Hanyuan County (Sichuan, China) and identified by Hanyuan Haoye Food Co., Ltd. The ZB samples were divided into three parts: stems of ZB (SZB), green seeds of ZB (GZB) and red seeds of ZB (RZB). The samples were subsequently subjected to washing and homogenization using cold phosphate-buffered saline (PBS). ZEVs from each part were extracted using differential centrifugation and ultrafiltration [23]. In the end, we get three kinds of ZEVs from SZB, GZB and RZB. The ZEVs were stored at −80 ℃.

2.2. ZEVs characterisation

ZEVs from SZB, GZB, and RZB were negatively stained with 2% phosphotungstic acid for 2 min and then analyzed by transmission electron microscopy (TEM, JEOL, Japan) for ultrastructural examination. ZEVs' diameter and concentration were assessed using a nanoparticle tracking analyzer (NTA, Meerbusch, Germany) with a 488 nm laser. The three ZEVs samples were tested, and the results showed that they are double-membrane vesicles with a particle size of 100–200 nm.

2.3. Cell culture

Zhongqiao Xinzhou Ltd. (Shanghai, China) has improved the LX-2 cells. Cells were cultured in Dulbecco's Modified Eagle Medium (DMEM, Gibco, USA) containing 10% fetal bovine serum (FBS, Biological Industries, Israel) and 1% penicillin-streptomycin. The cells were placed in a 37 ℃ incubator containing 5% CO_2.

2.4. Cellular uptake assays

Incubate LX-2 cells for 24 h after seeding the slides into 12-well plates. SZB, GZB, and RZB ZEVs (2×10^{10} particles/mL) were labeled with Dil (AAT Bioquest, USA) and subsequently added to the culture medium for a 24-hour incubation. The cells were fixed with 4% paraformaldehyde (Wako, Japan) and stained with 4',6-diamidino-2-phenylindole (DAPI, Biosharp, China). The uptake of ZEVs by LX-2 cells was observed by fluorescence microscopy (Leica Microsystems, Germany). The fluorescence signal intensity was subsequently quantified and analysed using ImageJ software.

2.5. Cell proliferation assay

LX-2 cells were seeded in a 96-well plate at a density of 5,000 cells per well and cultured for 12 h. Subsequently, ethanol (50, 100, 150, 200, 250, 300, 350, and 400 mmol/L) were added to the culture medium for 48 h. The absorbance measurements indicated that 100 mmol/L ethanol was effective in stimulating the proliferation of LX-2 cells.

Next, we evaluated the potential cytotoxic effects of ZEVs at different concentrations. LX-2 cells in 96-well plates were grouped into four: control and

ZEVs-treated groups using SZB, GZB and RZB. Addition of different concentrations of ZEVs (1×10^7, 1×10^8, 1×10^9, 2×10^9 particles/mL) to cells for 48 h. Depending on the results, we used ZEVs at a concentration of 2×10^9 particles/mL to treat the cells in subsequent experiments.

Then, cells were divided into 5 groups: negative control, positive control (ethanol, 100 mmol/L), and ZEVs of SZB, GZB and RZB. Subsequently, except for the negative control group, ethanol (100 mmol/L) and ZEVs (2×10^9 particles/mL) were added to the media of the corresponding groups for 48 h of incubation.

The viability of LX-2 cells was measured by Cell Counting Kit-8 (CCK-8, Biosharp, China) at 450 nm.

2.6. Cell scratching assay

When the LX-2 cells in 12-well plate have reached 90% density, a scratch was made on the monolayer using a 100 μL pipette tip. Serum-free medium was then added to prevent further cell proliferation. ZEVs of SZB, GZB, and RZB (2×10^9 particles/mL) were introduced into the culture medium and incubated for 24 h. Scratch images were captured at 0 h and 24 h using an optical microscope (Leica Microsystems, Germany). The migration area at 24 h was subtracted from the migration area at 0 h to calculate the migration distance. The relative migration rate was calculated using the formula: (migration area with ZEVs/migration area with PBS) × 100%.

2.7. Animal experiment

To investigate the effects of ZEVs in mice, we first assessed the biosafety *in vivo*. Twenty healthy male C57BL/6N mice (Charles River, China, 6–8 weeks old) were randomly assigned to four groups: control group and ZEVs of SZB, GZB, RZB groups. Previous experiments indicated no effect of 2×10^9 particles/mL ZEVs on LX-2 cell growth, considering the need for *in vivo* demonstration in mice. So, ZEVs of SZB, GZB and RZB (2×10^{10} particles/mL, 100 μL/pc) were administered by gavage for 7 days. Afterward, serum and visceral tissues (heart, liver, spleen, lung and kidney) were collected for liver function analysis, including ALT and AST measurements, as well as histological examination by H&E.

Then, 25 male C57BL/6N mice were used for liver fibrosis study [24–26]. The mice were randomly divided into 5 groups: (1) negative control group (control liquid diet), (2) positive control group (alcohol liquid diet + 31.5% alcohol gavage + PBS), (3) SZB group (alcohol liquid diet + 31.5% alcohol gavage + SZB ZEVs), (4) GZB group (alcohol liquid diet + 31.5% alcohol gavage + GZB ZEVs) and (5) RZB group (alcohol liquid diet + 31.5% alcohol gavage + RZB ZEVs). The negative control group was fed a Lieber-DeCarli control liquid diet (Trophic Animal Feed High-tech Co., Ltd, China) for 9 weeks. The remaining groups were fed a gradual transition from 1% to 5% (vol/vol) alcohol liquid diet (Trophic Animal Feed High-tech Co.,Ltd, China) in the first week and kept 8 weeks. Four groups of mice also received 31.5% alcohol (5 g/kg, twice a week) by gavage for 8 weeks. From week 5 to week 9, mice were gavaged with ZEVs (2×10^{10} particles/mL, 100 μL/pc, four times a week). Mice in the negative and positive control group were administered an

equivalent volume of PBS.

Following anesthesia, the mice were euthanized. The liver was excised and fixed in 4% formaldehyde for subsequent sectioning and staining. Serum samples were collected for biochemical analysis.

2.8. AST and ALT measurement

Automatic biochemical analyzer (Au5800, Beckman, USA) was used to measure the ALT and AST in mice serum to assess changes in liver function in mice from both experiments.

2.9. Hematoxylin-eosin (H&E), Masson and Oil Red O staining

Mice tissues were taken, fixed, dehydrated, embedded and made into 3μm sections for H&E and Masson. Fresh liver tissues were cut into 6μm thick slices by frozen sectioning and stored at −80 ℃ for Oil Red O. H&E (Biosharp, China), Masson (Solarbio, China) and Oil Red O (Biosharp, China) were performed according to the instructions. Then, light microscope (Nexcope, China) was used to observe morphological changes.

2.10. Western blotting

Cell or liver tissues total proteins were extracted with RIPA reagent, and BCA assay was used to measure the protein concentration. After the proteins were separated using SDS-PAGE, the proteins were transferred to a PVDF membranes (Millipore, USA) for detection. Subsequently, the PVDF membranes was closed in 5% non-fat milk for 1 h. They were then incubated overnight using primary antibodies, including diluted mouse anti-GAPDH (1: 5000; proteintech, China), mouse anti-β-tubulin (1: 2000; proteintech, China), mouse anti-COL I (1: 1000; proteintech, China), rabbit anti-α-SMA (1: 500; proteintech, China). Incubate the membranes with species-specific secondary antibodies (1: 5000; proteintech, China) conjugated to horseradish peroxidase for 2 h. Visualization was performed using a chemiluminescent substrate (Millipore, USA).

2.11. Real-time PCR assays

LX-2 cells in 6-well plates were divided into 5 groups: negative control, positive control, and ZEVs of SZB, GZB and RZB. After the cells have stabilized, ethanol (200 mmol/L) and ZEVs of SZB, GZB and RZB (2×10^9 particles/mL) were added to the culture medium for co-cultivation for 48 h.

LX-2 cells were lysed by Trizol reagent (Vazyme, China) to extract total RNA, followed by reverse transcription of total RNA to cDNA using the vazyme RT SuperMix Kit (Vazyme, China). cDNA obtained was added to the SYBR quantitative PCR (qPCR) mix and real-time PCR was performed on a qPCR instrument (Roche, Switzerland). The primers used are shown in Supplementary **Table S1**. The following cycling conditions were used: initial denaturation at 94 ℃ for 3 min, followed by 40 cycles at 94 ℃ for 15 s, and 60 ℃ for 30 s. Using GAPDH as the internal reference, the $2^{-\Delta\Delta Ct}$ method was used to calculate the expression levels of target genes.

2.12. Sequencing and preparation of the ZEVs miRNA library

RNA extracted from ZEVs of SZB, GZB and RZB using HiPure Exosome RNA Kit (Magen, China). The miRNA Kit (Bio Scientific Corporation, USA) was used to prepare a library from 10 ng of miRNA. In an unbiased reaction, adaptors are coupled to the miRNA's 3' and 5' ends. The cDNAs were produced by reverse transcription of miRNAs with an adapter. Huayin Ltd. (Guangzhou, China) built and sequenced the cDNA library.

2.13. Cell transfection

LX-2 cells were divided into 5 groups: negative control, positive control, miR-NC (a miR for control), miR-9 and miR-17. Mixed transfection reagents (Transgen, China) and miR-NC, miR-9 or miR-17 were added and cultured for 8 h, then the cells were incubated with DMEM containing ethanol (200 mmol/L) for 48 h. After that, cellular proteins were measured by western blotting.

2.14. Quantification and statistical analysis

The analysis of all data was performed using GraphPad Prism 8.0.2 software, employing One-way ANOVA. A *P*-value of less than 0.05 was deemed statistically significant. The results are derived from three independent experiments.

3. Results

3.1. Characterization of ZEVs

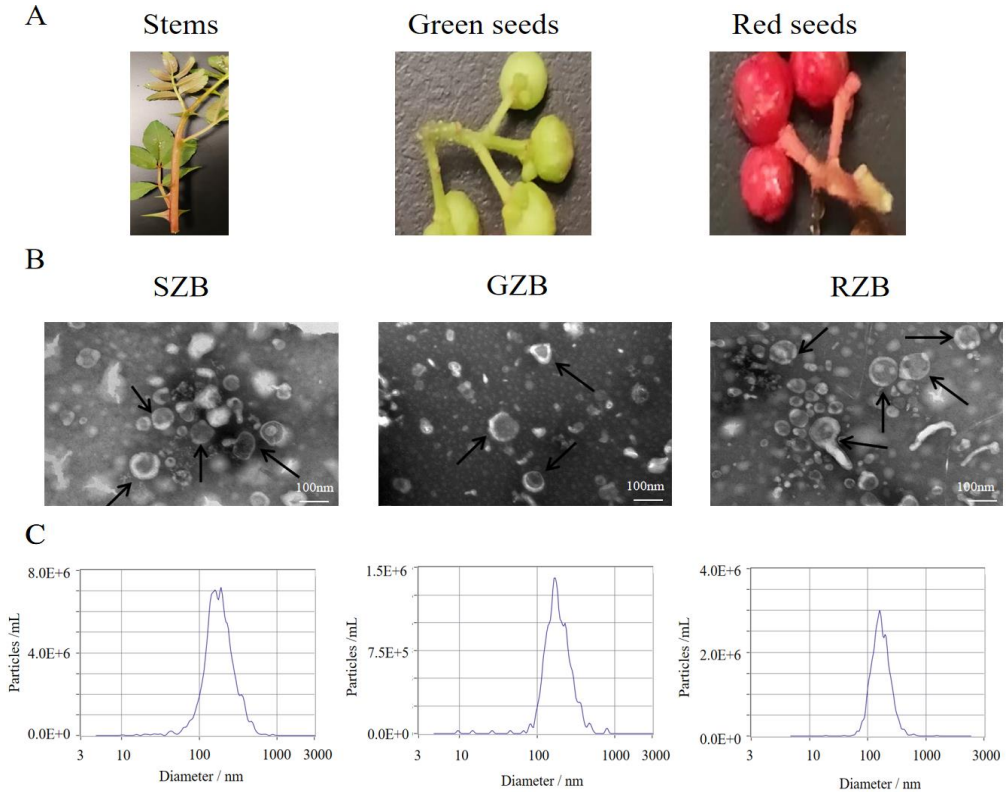

Figure 1. Characterization of ZEVs **(A)** Three different parts of ZB; **(B)** TEM of ZEVs. representative ZEVs are shown by black arrows. Scale bar = 100 nm. Magnification: 120000X; **(C)** NTA of ZEVs.

We isolated ZEVs from three components of ZB, namely SZB, GZB and RZB, using a combination of differential centrifugation and ultrafiltration (**Figure 1A**). TEM analysis revealed that ZEVs were double-membrane vesicles with sizes ranging from 100 to 200 nm (**Figure 1B**). NTA was then employed to assess the size distribution of ZEVs. The average sizes of ZEVs derived from SZB, GZB, and RZB were 173.8 nm, 176.9 nm, and 161.6 nm, respectively (**Figure 1C**).

3.2. Cellular uptake assays

After co-incubation of LX-2 cells with Dil-labeled ZEVs, it was observed that ZEVs from all three sources accumulated in the cytoplasm of the cells (**Figure 2A,B**), confirming successful uptake of ZEVs by LX-2 cells. (Error bar represents SD; $n = 3$; $^{**}P < 0.01$, indicating a significant difference from the control group).

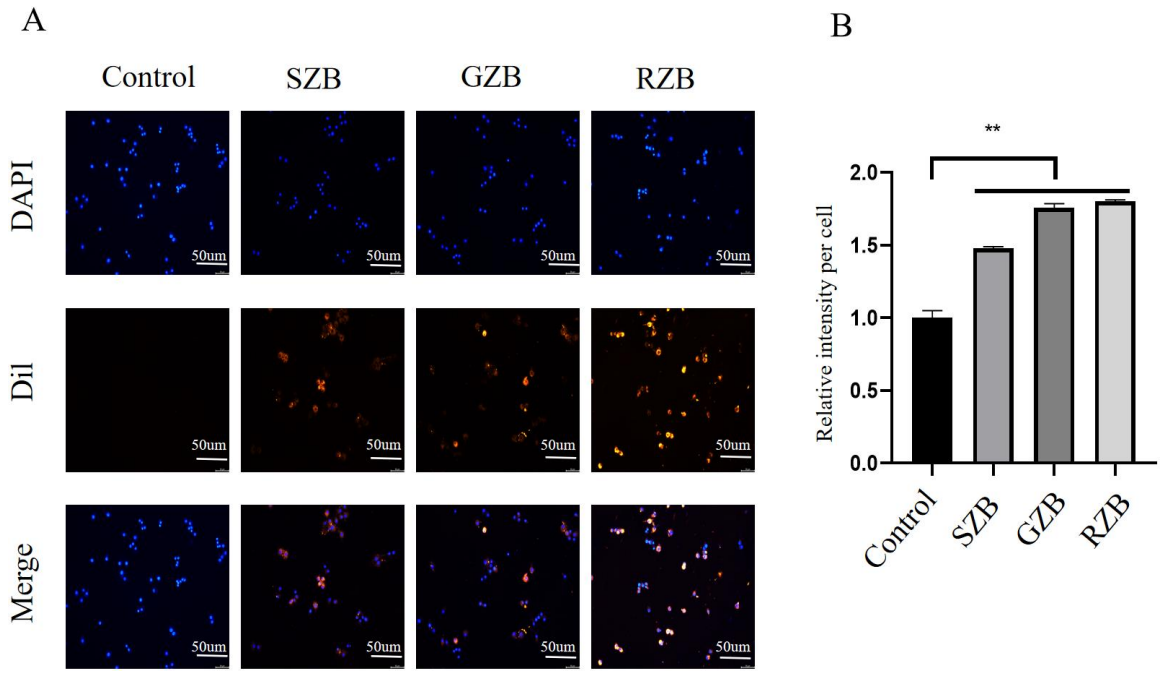

Figure 2. LX-2 cells intake of ZEVs **(A)** Fluorescence microscope pictures of ZEVs being taken up by cells. Scale bars = 50 μm. Magnification: 200X; **(B)** Quantification of fluorescence intensity.

3.3. Effects of ethanol on LX-2 cells proliferation and protein expression

Acetaldehyde, the primary active metabolite of ethanol, has been shown to activate rat HSCs and increase the expression of fibrosis-associated proteins, including α-SMA and COL I [27]. Based on this, we hypothesized that ethanol could similarly activate LX-2 cells. To verify this, we examined LX-2 cells viability with CCK-8 after 48 h of action with ethanol. The results indicated that 50, 100, 150, and 200 mmol/L ethanol concentrations promoted LX-2 cells proliferation, with the most significant effect observed at 100 mmol/L (**Figure 3A**). Furthermore, cellular protein was analyzed under the influence of ethanol. The results revealed that the use of 200 mmol/L ethanol induced COL I and α-SMA expression in LX-2 cells (**Figure 3B**). (Error bar represents SD; $n = 3$; $^{**}P < 0.01$, indicating a significant difference from the control group).

3.4. Suppression of LX-2 cells proliferation by ZEVs

We assessed the effects of SZB, GZB, and RZB ZEVs on cell proliferation. LX-2 cells were exposed to each ZEV types (1×10^7, 1×10^8, 1×10^9, 2×10^9 particles/mL). The results indicated that none of the ZEVs concentrations affected cell growth (**Figure 3C–E**). Additionally, treatment with 2×10^9 particles/mL ZEVs had no impact on LX-2 cell growth and showed no cytotoxic effects (**Figure 3F**). Consequently, we selected 2×10^9 particles/mL ZEVs for subsequent experiments. Absorbance at 450 nm was measured after addition of ZEVS and ethanol to the cells for 48 h. The results indicated that ethanol induced LX-2 cells proliferation, whereas ZEVs significantly reduced the proliferation of ethanol-activated LX-2 cells (**Figure 3G**). (Error bar represents SD; $n = 3$; $^{ns}P > 0.05$, indicating no significant difference from the control group. $^{**}P < 0.01$, indicating a significant difference from the positive control group).

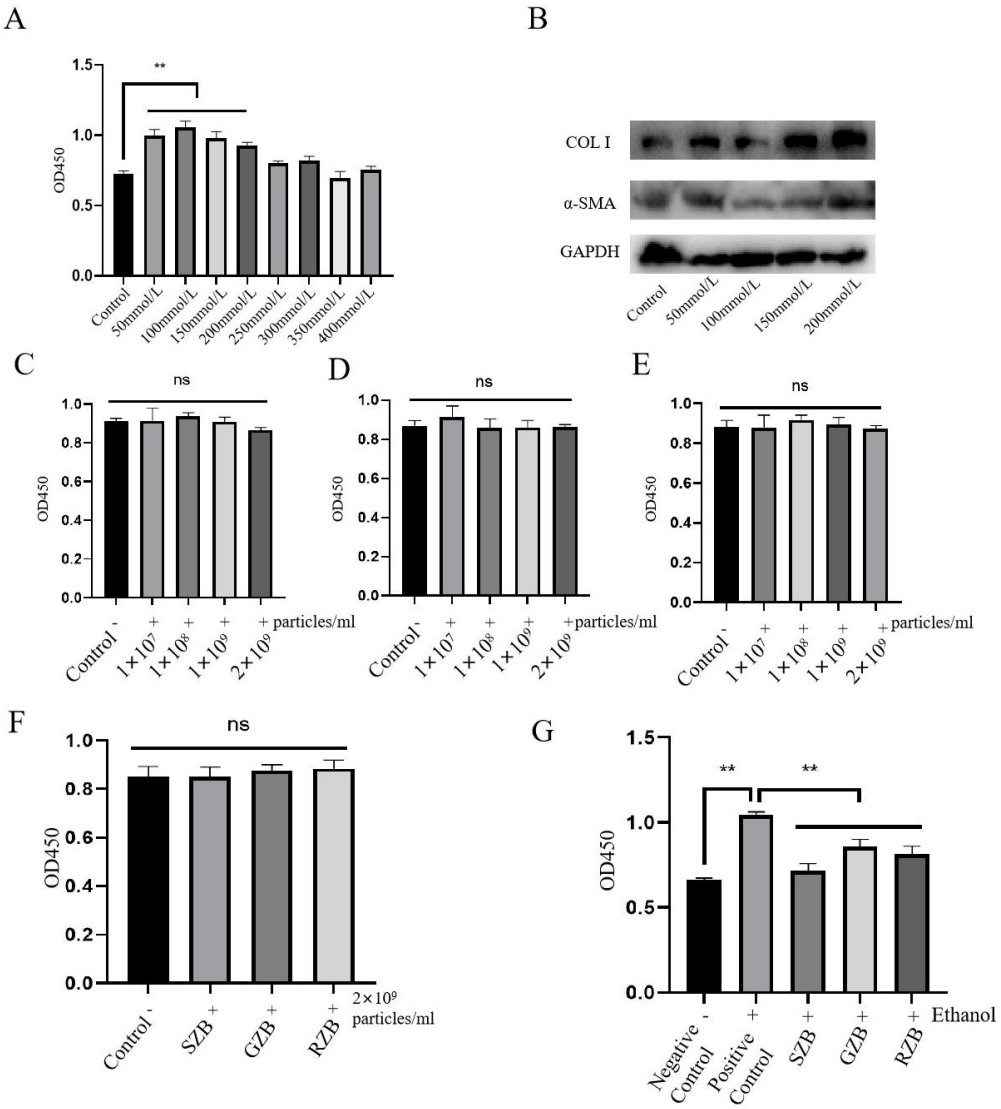

Figure 3. Effects of ethanol or ZEVs in LX-2 cells **(A)** Absorbance at 450 nm of LX-2 cells; **(B)** Western blotting analysis of COL I and α-SMA; **(C–E)** Effect of SZB, GZB and RZB concentration gradient on non-activated LX-2 cells; **(F)** Proliferative effects of ZEVs on non-activated LX-2 cells; **(G)** Inhibitory effect of ZEVs on proliferation of activated LX-2 cells.

3.5. Effect of ZEVs on fibrotic proteins in activated LX-2 cells

COL I and α-SMA, hallmark proteins of fibrosis, were detected in LX-2 cells [28]. As shown in **Figure 4A–F**, compared to negative control, ethanol was able to significantly elevate the gene and protein levels of COL I and α-SMA in LX-2 cells.

However, upon treatment with ZEVs, the elevated gene and protein levels were partially reduced. These results suggest that ZEVs can decrease the content of fibrotic proteins in activated LX-2 cells, indicating their potential anti-fibrotic effect. (Error bar represents SD; $n = 3$; $^{**}P < 0.01$, indicating significantly different from positive control group).

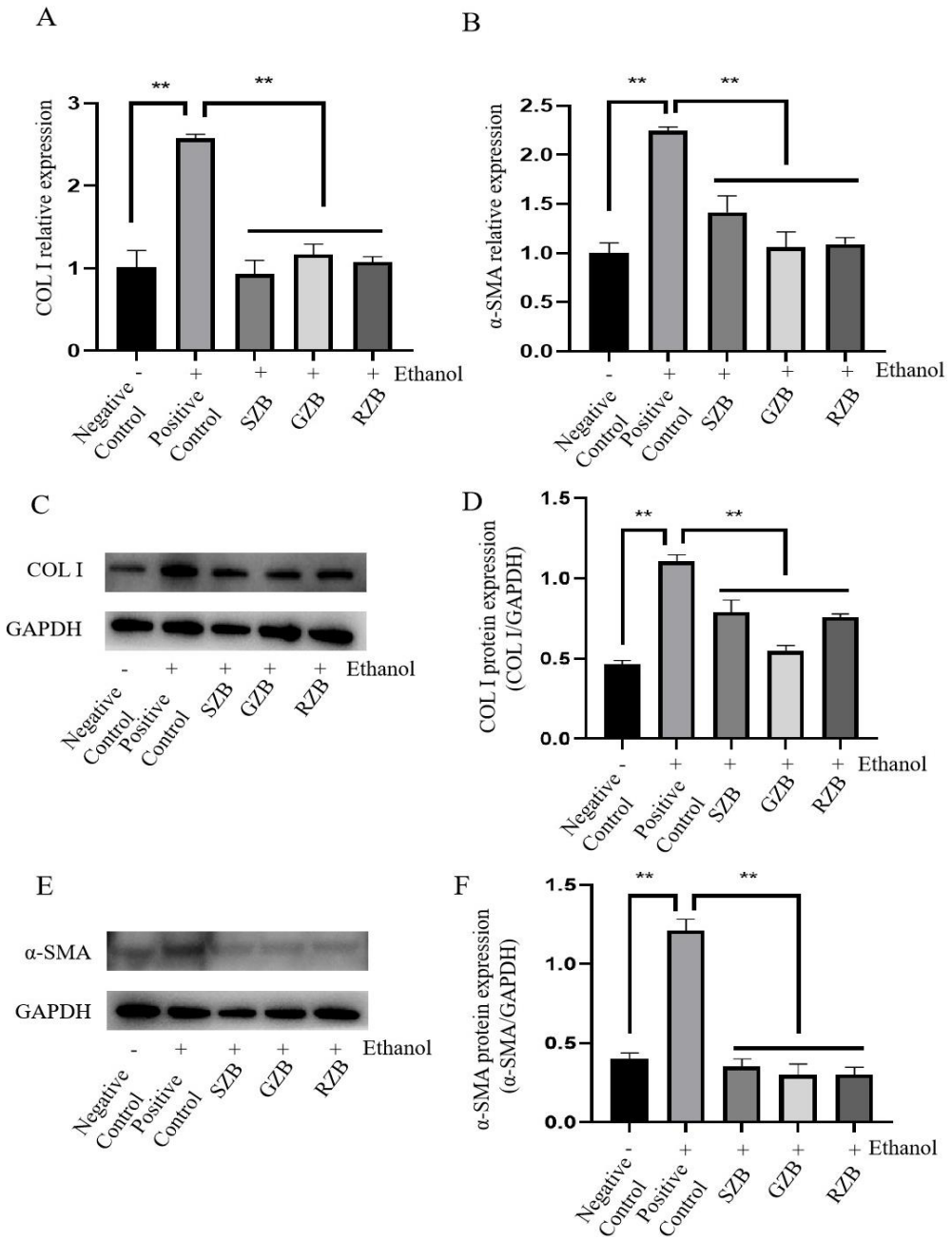

Figure 4. Effect of ZEVs on fibrotic proteins in activated LX-2 cells **(A–B)** Real-time PCR analysis of COL I and α-SMA; **(C)** Western blotting analysis of COL I; **(D)** Quantification of COL I; **(E)** Western blotting analysis of α-SMA; **(F)** Quantification of α-SMA.

3.6. Effect of ZEVs on cell migration

The migration of LX-2 cells is a key event in the progression of hepatic fibrosis [29]. To assess the potential of SZB, GZB and RZB ZEVs in inhibiting cell motility, scratch wound healing test was used to explore. Serum-free medium was added at 0 h to inhibit cell proliferation [30]. The results show that ZEVs were able to reduce the migratory area of LX-2 cells (**Figure 5A,B**). Furthermore, compared to the control group, the gene expression of MMP-9, a member of the matrix metalloproteinase (MMP) family implicated in cell migration and invasion [31], was significantly reduced following ZEVs treatment (**Figure 5C**). These results show that ZEVs may exert antifibrotic effects by inhibiting LX-2 cells migration. (Error bar represents SD; n = 3; **P < 0.01, indicating significantly different from control group).

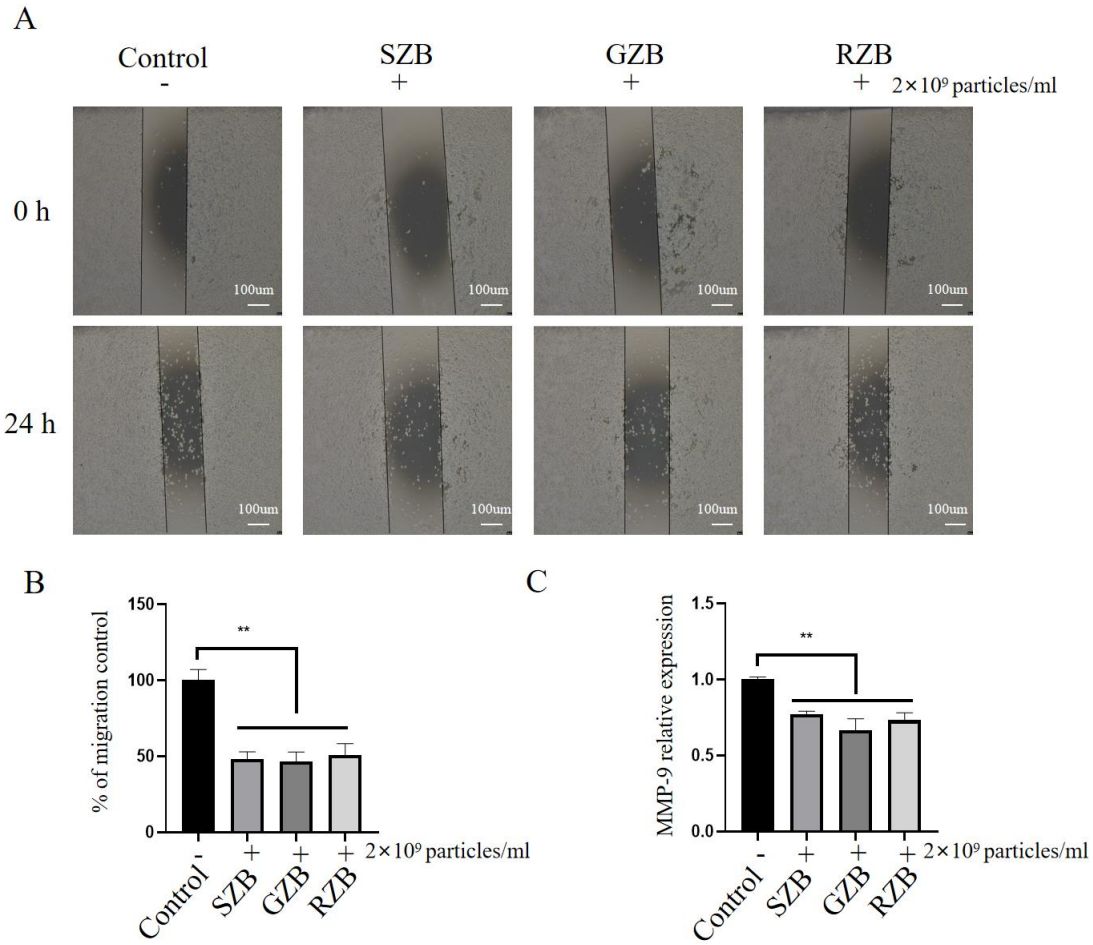

Figure 5. Effect of ZEVs on cell migration **(A)** The edges of the scratches are marked with a black line. Scale bar = 100 μm. Magnification: 40X; **(B)** Quantification of wound area shown in **(A)**; **(C)** Real-time PCR analysis of MMP-9.

3.7. Biosafety of ZEVs *in vivo*

To assess the safety of orally administered SZB, GZB and RZB ZEVs, serum sample and major organs (heart, liver, spleen, lung and kidney) were collected from mice that were administered 2×10^{10} particles/mL (100 μL/pc) of ZEVs for 7 days (**Figure 6A**). There were no significant changes in ALT and AST levels between the control group and the ZEVs-treated group (**Figure 6B,C**). In addition, histological

examination of the major organs by H&E revealed that there were no obvious signs of abnormality or damage in the organs of the mice in the ZEVs-treated group (**Figure 6D**). (Error bar represents SD; $n = 3$; $^{ns}P > 0.05$, indicating no significantly different from control group).

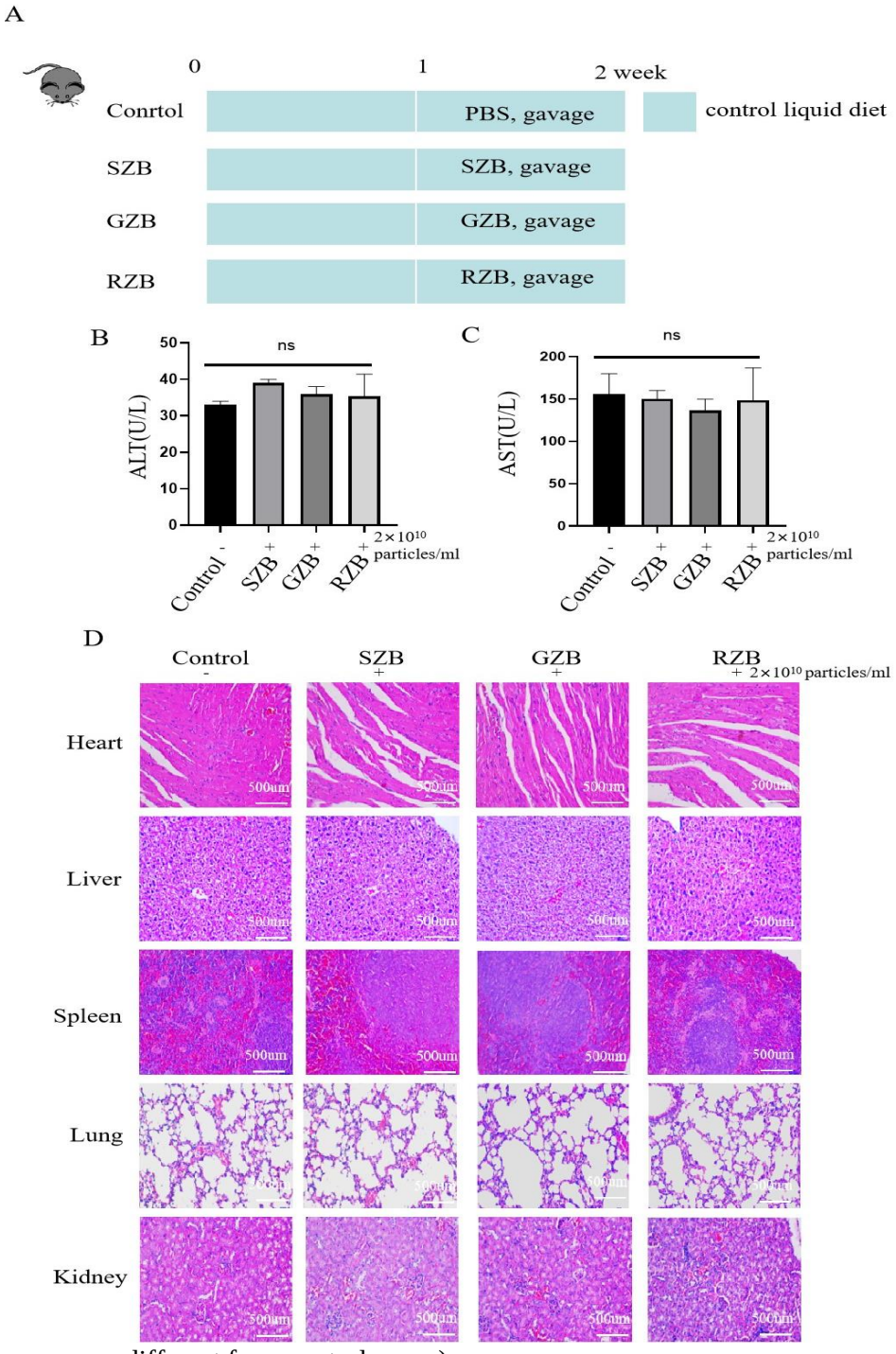

Figure 6. Biosafety of ZEVs in mice **(A)** Schematic handling of *in vivo* biosafety assessment; **(B,C)** ALT and AST levels in the serum of mice; **(D)** H&E of major organs. Scale bar = 500 μm. Magnification: 400X.

3.8. ZEVs alleviate liver fibrosis in mice

To investigate the treatment effect of ZEVs on liver fibrosis, we established mice model of alcoholic liver fibrosis (**Figure 7A**). H&E revealed that the alcohol

liquid diet and alcohol treatment induced inflammatory cell infiltration and morphological changes in liver lobules, which were significantly improved following oral ZEVs administration (**Figure 7B**). Masson showed that, compared to the positive control group, ZEVs treatment markedly reduced collagen deposition around the central veins and portal areas of liver tissue (**Figure 7C**). Oil red O showed that ZEVs was able to reduce lipid droplet deposition in liver tissue of hepatic fibrosis mice (**Figure 7D**). Furthermore, compared with the positive control group, oral administration of ZEVs reduced serum levels of ALT and AST (**Figure 7E,F**), as well as, COL I and α-SMA protein expression in liver tissues (**Figure 7G–J**). (Error bar represents SD; n = 3; $^{**}P < 0.01$, indicating significantly different from positive control group).

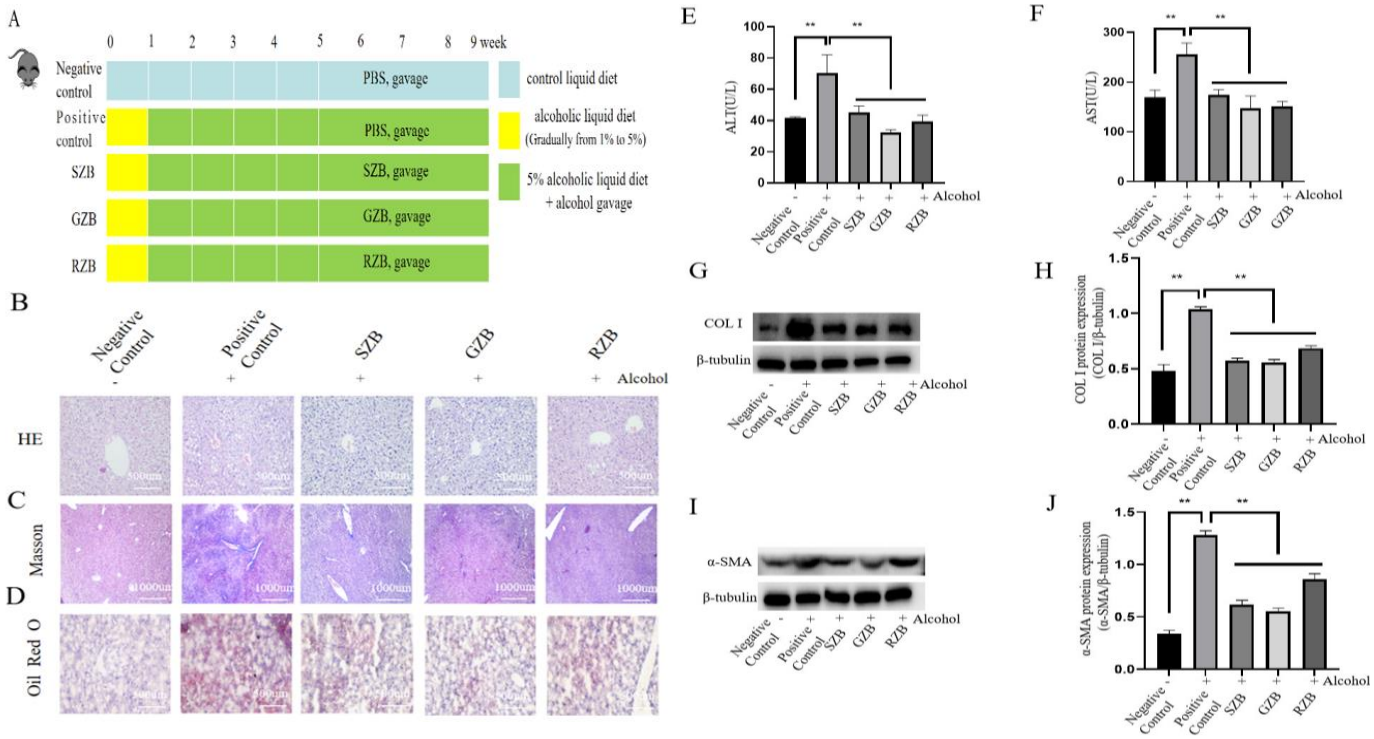

Figure 7. The effect of ZEVs on liver fibrosis mice **(A)** Process of treating mice; **(B)** H&E of livers. Scale bar = 500 μm. Magnification: 400X; **(C)** Masson of livers. Scale bar = 1000 μm. Magnification: 100X; **(D)** Oil Red O of livers. Scale bar = 500 μm. Magnification: 400X; **(E,F)** ALT and AST levels in the serum; **(G)** Western blotting analysis of COL I; **(H)** Quantification of COL I; **(I)** Western blotting analysis of α-SMA; **(J)** Quantification of α-SMA.

3.9. ZEVs regulate the TGF-β1/Smad signaling pathway in activated LX-2 cells

Activation of HSCs is an important factor in the process of liver fibrosis, and TGF-β1/Smad is the main signalling pathway that stimulates HSCs activation [32]. According to real-time PCR analysis, ZEVs can significantly reduce the expression of TGF-β1, Smad2, and Smad3 in activated LX-2 cells compared to the positive control (**Figure 8A–C**). These observations demonstrated that ZEVs could effectively disrupt the TGF-β1/Smad signaling pathway. (Error bar represents SD; n = 3; $^{*}P < 0.05$, $^{**}P < 0.01$, indicating significantly different from positive control group).

3.10. MiR-9 and miR-17 in ZEVs were shown to decrease liver fibrosis

EVs contain a wide array of components, including proteins, lipids, nucleic acids, and other compounds, with miRNAs garnering significant attention due to their functional and therapeutic relevance. For instance, miR-44 in tea has been shown to reduces COL I and α-SMA expression levels in LX-2 cells [17]. Furthermore, miRNAs generated from ginger extracellular vesicle-like nanoparticles were discovered to block the expression of SARS-CoV-2 genes [33]. To investigate whether miRNAs from ZEVs exert an anti-fibrotic effect, we identified 28, 103, and 31 miRNAs with lengths ranging from 18 to 24 nt in SZB, GZB and RZB ZEVs, respectively. Notably, miR-9 and miR-17 were highly expressed in all three ZEVs, and were selected for further investigation (Supplementary **Table S2**). MiR-NC, miR-9 and miR-17 were transfected into LX-2 cells, which were subsequently cultured in ethanol-containing (200 mmol/L) DMEM for 48 h. Western blotting results demonstrated a reduction in COL I and α-SMA levels in the transfected cells compared to the positive control (**Figure 8D,E**). These results demonstrated that miR-9 and miR-17 have potential anti-fibrotic effects in liver fibrosis.

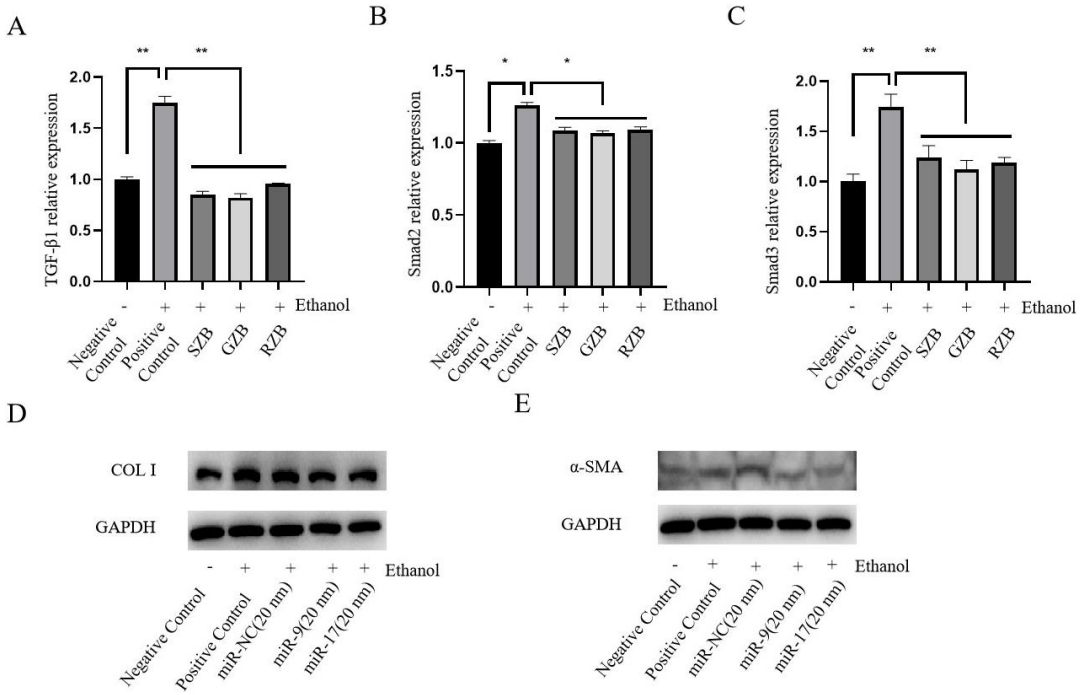

Figure 8. The effects of ZEVs or miRNAs in activated LX-2 cells **(A–C)** Real-time PCR analysis of TGF-β1, Smad2 and Smad3; **(D)** The effect of miRNAs on cellular COL I protein; **(E)** The effect of miRNAs on cellular α-SMA protein.

4. Discussion

Liver fibrosis is a wound-healing reaction against chronic liver damage, resulting from the disruption of ECM [34]. In the progression of liver fibrosis, aHSCs differentiate into myofibroblasts, which are the main driving factor of liver fibrosis [5]. Upon activation, qHSCs lose their characteristic cytoplasmic lipid droplets and transform into aHSCs. These aHSCs then differentiate into myofibroblasts, which are responsible for synthesizing collagen and ECM structural

glycoproteins [35]. Therefore, the main target of treating liver fibrosis is to inhibit the activation of HSCs.

ZB, a plant with both medicinal and culinary uses, has a history of millennia in China. Researches have revealed that ZB contains a diversity of bioactive compounds with antiparasitic, antibacterial, anti-inflammatory, and antioxidant properties [20]. To explore the potential anti-liver fibrosis effects of ZB, we first extracted ZEVs from ZB, which upon characterization displayed a double-membrane structure and a size ranging from 100 to 200 nm. Next, we assessed the cellular uptake of ZEVs and their potential cytotoxicity. The findings revealed that LX-2 cells efficiently internalized the ZEVs with no significant toxicity. Subsequently, we examined the treatment efficacy of ZEVs for hepatic fibrosis. *In vitro*, ZEVs inhibited the propliferation of activated LX-2 cells, suppressed the cell migration capacity in serum-free medium, and reduced COL I and α-SMA in LX-2 cells. *In vivo*, we first investigated the biosafety of ZEVs in normal mice, and the H&E results showed that ZEVs no damage to the heart, liver, spleen, lung and kidney of mice. Furthermore, ZEVs reduced the ALT and AST levels in liver fibrosis mice, decreased lipid droplet accumulation and collagen deposition in liver tissues, and lowered the α-SMA and COL I protein. Animal models do not fully reflect human disease, so ZEVs need to be explored for a long time before they can be used in the clinic [36]. In summary, these findings suggest that ZEVs possess anti-fibrotic effects.

We delved into the specific mechanisms of ZEVs against liver fibrosis. Researchers have found that platelet-derived growth factor (PDGF), transforming growth factor-beta (TGF-β), WNT/β-catenin signaling, and the NLRP3-Caspase1 pathway are important pathways associated with HSC activation and fibrosis [37–39]. Moreover, the development of liver fibrosis in both alcoholic fatty liver disease (ALD) and NAFLD shares common mechanisms. In the context of fatty acid oxidation, downstream signaling events of transcription factor-regulated genes involved in lipid synthesis and endoplasmic reticulum (ER) stress response are present in both NAFLD and ALD [40]. Among these, TGF-β1 is the most effective cytokine in promoting HSC activation and proliferation [41]. The “SMAD” protein family, as downstream signaling molecules of TGF-β1, also plays a significant function in the progression of liver fibrosis. Upon binding of TGF-β1 to its receptor, it activates downstream signaling pathways, promoting the phosphorylation of Smad2 and Smad3, which then bind to Smad4 and enter the nucleus to mediate fibrosis, whereas Smad7 negatively regulates signaling through the ubiquitin-proteasome degradation pathway [42,43]. Finally, we observed a decrease in gene expression levels of TGF-β1, Smad2 and Smad3 in activated LX-2 cells after treatment with ZEVs. These observations demonstrate that ZEVs can regulate the TGF-β1/Smad pathway.

To identify specific active components in ZEVs responsible for anti-hepatic fibrosis effects, we performed miRNA sequencing on ZEVs. The results showed that ZEVs were enriched in miR-9 and miR-17. We then synthesized these miRNAs and transfected them into activated LX-2 cells. Protein analysis showed that transfection of miR-9 and miR-17 into LX-2 cells significantly reduced the expression of COL I and α-SMA. These results suggest that miR-9 and miR-17 possess anti-liver fibrosis

activity. Future studies should investigate whether miRNAs from ZEVs are absorbed by the intestine and exert protective effects against liver fibrosis in consumers.

5. Conclusion

In this study, we confirmed that ZEVs were not significantly toxic to LX-2 cells and mice. ZEVs inhibited the proliferation and migration of LX-2 cells, while modulating the levels of fibrosis-related proteins and regulating the TGF-β1/Smad pathway. Furthermore, ZEVs mitigated liver damage in mice with hepatic fibrosis by reducing inflammatory cell infiltration, collagen deposition, and lipid droplet accumulation, as well as downregulating the expression of fibrosis-related proteins. Collectively, our findings suggest that ZEVs exhibit therapeutic effects in the treatment of liver fibrosis.

Supplementary materials: Supplementary **Table S1** shows the primer sequences used for LX-2 cells. Supplementary **Table S2** shows the sequencing results of microRNAs in ZEVs.

Author contributions: Conceptualization, YG; methodology, TJ; software, RF; validation, RF, BZ and JX; formal analysis, TJ and NP; investigation, BZ and JX; resources, MZ; data curation, MZ and NP; writing—original draft preparation, TJ; writing—review and editing, QG; visualization, QG; supervision, YG; project administration, YG; funding acquisition, QG and YG. All authors have read and agreed to the published version of the manuscript.

Funding: Our work was supported by the Foundation of Sichuan Science and Technology Program (24NSFSC1611), the Third People's Hospital of Chengdu Clinical Research Program (CSY-YN-01-2023-065 and CSY-YN-03-2024-015) and Chengdu Medical Research Project Foundation (2022284).

Ethical approval: The study was conducted in accordance with the Declaration of Helsinki, and was reviewed and approved by Ethics Committee of Southwest Jiaotong University with the approval number: SWJTU-2203-NSFC (026), dated 14 March 2022.

Data availability statement: The miRNA raw sequence data reported in our study have been deposited in https://ngdc.cncb.ac.cn/gsa (repository name: Genome Sequence Archive in National Genomics Data Center, accession number: CRA012608).

Conflict of interest: The authors declare no conflict of interest.

References

1. Qin L, Qin J, Zhen X, et al. Curcumin protects against hepatic stellate cells activation and migration by inhibiting the CXCL12/CXCR4 biological axis in liver fibrosis: A study in vitro and in vivo. Biomedicine & Pharmacotherapy. 2018; 101: 599-607. doi: 10.1016/j.biopha.2018.02.091
2. Kisseleva T, Brenner DA. Mechanisms of Fibrogenesis. Experimental Biology and Medicine. 2008; 233(2): 109–122. doi: 10.3181/0707-mr-190
3. Elpek GÖ. Cellular and molecular mechanisms in the pathogenesis of liver fibrosis: An update. World Journal of Gastroenterology. 2014; 20(23): 7260. doi: 10.3748/wjg.v20.i23.7260

4. Qin DM, Zhang Y, Li L. Progress in research of Chinese herbal medicines with anti-hepatic fibrosis activity. World Chinese Journal of Digestology. 2017; 25(11): 958. doi: 10.11569/wcjd.v25.i11.958
5. Higashi T, Friedman SL, Hoshida Y. Hepatic stellate cells as key target in liver fibrosis. Advanced Drug Delivery Reviews. 2017; 121: 27–42. doi: 10.1016/j.addr.2017.05.007
6. Aydin MM, Akcali KC. Liver fibrosis. The Turkish Journal of Gastroenterology. 2018; 29(1): 14–21. doi: 10.5152/tjg.2018.17330
7. Zhang CY, Yuan WG, He P, et al. Liver fibrosis and hepatic stellate cells: Etiology, pathological hallmarks and therapeutic targets. World Journal of Gastroenterology. 2016; 22(48): 10512. doi: 10.3748/wjg.v22.i48.10512
8. Li D, He L, Guo H, et al. Targeting activated hepatic stellate cells (aHSCs) for liver fibrosis imaging. EJNMMI Research. 2015; 5(1). doi: 10.1186/s13550-015-0151-x
9. Puche JE, Saiman Y, Friedman SL. Hepatic Stellate Cells and Liver Fibrosis. Comprehensive Physiology. 2013; 3(4): 1473–1492. doi: 10.1002/cphy.c120035
10. Wang FD, Zhou J, Chen EQ. Molecular Mechanisms and Potential New Therapeutic Drugs for Liver Fibrosis. Frontiers in Pharmacology. 2022; 13. doi: 10.3389/fphar.2022.787748
11. Xu L. Human hepatic stellate cell lines, LX-1 and LX-2: new tools for analysis of hepatic fibrosis. Gut. 2005; 54(1): 142–151. doi: 10.1136/gut.2004.042127
12. Xu S, Chen Y, Miao J, et al. Esculin inhibits hepatic stellate cell activation and CCl4-induced liver fibrosis by activating the Nrf2/GPX4 signaling pathway. Phytomedicine. 2024; 128: 155465. doi: 10.1016/j.phymed.2024.155465
13. Simons M, Raposo G. Exosomes—vesicular carriers for intercellular communication. Current Opinion in Cell Biology. 2009; 21(4): 575–581. doi: 10.1016/j.ceb.2009.03.007
14. Zhuang X, Deng Z, Mu J, et al. Ginger-derived nanoparticles protect against alcohol-induced liver damage. Journal of Extracellular Vesicles. 2015; 4(1). doi: 10.3402/jev.v4.28713
15. Gao Q, Chen N, Li B, et al. Natural lipid nanoparticles extracted from Morus nigra L. leaves for targeted treatment of hepatocellular carcinoma via the oral route. Journal of Nanobiotechnology. 2024; 22(1). doi: 10.1186/s12951-023-02286-3
16. Zhang L, He F, Gao L, et al. Engineering Exosome-Like Nanovesicles Derived from Asparagus cochinchinensis Can Inhibit the Proliferation of Hepatocellular Carcinoma Cells with Better Safety Profile. International Journal of Nanomedicine. 2021; Volume 16: 1575–1586. doi: 10.2147/ijn.s293067
17. Gong Q, Zeng Z, Jiang T, et al. Anti-fibrotic effect of extracellular vesicles derived from tea leaves in hepatic stellate cells and liver fibrosis mice. Frontiers in Nutrition. 2022; 9. doi: 10.3389/fnut.2022.1009139
18. Park SM, Kim JK, Kim EO, et al. Hepatoprotective Effect of Pericarpium zanthoxyli Extract Is Mediated via Antagonism of Oxidative Stress. Da Silva Filho AA, ed. Evidence-Based Complementary and Alternative Medicine. 2020; 2020(1). doi: 10.1155/2020/6761842
19. Wagner EBH, Bauer R, Melchart D, et al. Chromatographic Fingerprint Analysis of Herbal Medicines. Springer Vienna; 2011.
20. Zhou M, Shi F, Chen K, et al. Research progress of the medicinal value of Zanthoxylum bungeanum Maxim. Farm Products Processing. 2020; 495: 65–72.
21. Huang X, Yuan Z, Liu X, et al. Integrative multi-omics unravels the amelioration effects of Zanthoxylum bungeanum Maxim. on non-alcoholic fatty liver disease. Phytomedicine. 2023; 109: 154576. doi: 10.1016/j.phymed.2022.154576
22. Peng W, He CX, Li RL, et al. Zanthoxylum bungeanum amides ameliorates nonalcoholic fatty liver via regulating gut microbiota and activating AMPK/Nrf2 signaling. Journal of Ethnopharmacology. 2024; 318: 116848. doi: 10.1016/j.jep.2023.116848
23. Zu M, Xie D, Canup BSB, et al. 'Green' nanotherapeutics from tea leaves for orally targeted prevention and alleviation of colon diseases. Biomaterials. 2021; 279: 121178. doi: 10.1016/j.biomaterials.2021.121178
24. Qiu P, Mi A, Hong C, et al. An integrated network pharmacology approach reveals that Ampelopsis grossedentata improves alcoholic liver disease via TLR4/NF-κB/MLKL pathway. Phytomedicine. 2024; 132: 155658. doi: 10.1016/j.phymed.2024.155658
25. Khanova E, Wu R, Wang W, et al. Pyroptosis by caspase11/4-gasdermin-D pathway in alcoholic hepatitis in mice and patients. Hepatology. 2018; 67(5): 1737–1753. doi: 10.1002/hep.29645
26. Avila MA, Dufour JF, Gerbes AL, et al. Recent advances in alcohol-related liver disease (ALD): summary of a Gut round table meeting. Gut. 2019; 69(4): 764–780. doi: 10.1136/gutjnl-2019-319720

27. Wu X, Liu X qi, Liu Z ni, et al. CD73 aggravates alcohol-related liver fibrosis by promoting autophagy mediated activation of hepatic stellate cells through AMPK/AKT/mTOR signaling pathway. International Immunopharmacology. 2022; 113: 109229. doi: 10.1016/j.intimp.2022.109229
28. Brenner DA, Kisseleva T, Scholten D, et al. Origin of myofibroblasts in liver fibrosis. Fibrogenesis & Tissue Repair. 2012; 5(S1). doi: 10.1186/1755-1536-5-s1-s17
29. Du X, Hua R, He X, et al. Echinococcus granulosus ubiquitin-conjugating enzymes (E2D2 and E2N) promote the formation of liver fibrosis in TGF-β1-induced LX-2 cells. Parasit Vectors. 2024;17(1):190. doi:10.1186/s13071-024-06222-8.
30. Grada A, Otero-Vinas M, Prieto-Castrillo F, et al. Research Techniques Made Simple: Analysis of Collective Cell Migration Using the Wound Healing Assay. Journal of Investigative Dermatology. 2017; 137(2): e11–e16. doi: 10.1016/j.jid.2016.11.020
31. Itoh Y. MT1-MMP: A key regulator of cell migration in tissue. IUBMB Life. 2006; 58(10): 589–596. doi: 10.1080/15216540600962818
32. Friedman SL. Mechanisms of Hepatic Fibrogenesis. Gastroenterology. 2008; 134(6): 1655–1669. doi: 10.1053/j.gastro.2008.03.003
33. Teng Y, Xu F, Zhang X, et al. Plant-derived exosomal microRNAs inhibit lung inflammation induced by exosomes SARS-CoV-2 Nsp12. Molecular Therapy. 2021; 29(8): 2424–2440. doi: 10.1016/j.ymthe.2021.05.005
34. Parola M, Pinzani M. Liver fibrosis: Pathophysiology, pathogenetic targets and clinical issues. Molecular Aspects of Medicine. 2019; 65: 37–55. doi: 10.1016/j.mam.2018.09.002
35. Dewidar B, Meyer C, Dooley S, et al. TGF-β in Hepatic Stellate Cell Activation and Liver Fibrogenesis—Updated 2019. Cells. 2019; 8(11): 1419. doi: 10.3390/cells8111419
36. Gao B, Xu MJ, Bertola A, et al. Animal Models of Alcoholic Liver Disease: Pathogenesis and Clinical Relevance. Gene Expression. 2017; 17(3): 173–186. doi: 10.3727/105221617x695519
37. Ying HZ, Chen Q, Zhang WY, et al. PDGF signaling pathway in hepatic fibrosis pathogenesis and therapeutics. Molecular Medicine Reports. 2017; 16(6): 7879–7889. doi: 10.3892/mmr.2017.7641
38. Xu F, Liu C, Zhou D, et al. TGF-β/SMAD Pathway and Its Regulation in Hepatic Fibrosis. Journal of Histochemistry & Cytochemistry. 2016; 64(3): 157–167. doi: 10.1369/0022155415627681
39. Nishikawa K, Osawa Y, Kimura K. Wnt/β-Catenin Signaling as a Potential Target for the Treatment of Liver Cirrhosis Using Antifibrotic Drugs. International Journal of Molecular Sciences. 2018; 19(10): 3103. doi: 10.3390/ijms19103103
40. Tarantino G, Citro V. What are the common downstream molecular events between alcoholic and nonalcoholic fatty liver? Lipids in Health and Disease. 2024; 23(1). doi: 10.1186/s12944-024-02031-1
41. Derynck R, Zhang YE. Smad-dependent and Smad-independent pathways in TGF-β family signalling. Nature. 2003; 425(6958): 577–584. doi: 10.1038/nature02006
42. Fukasawa H, Yamamoto T, Togawa A, et al. Down-regulation of Smad7 expression by ubiquitin-dependent degradation contributes to renal fibrosis in obstructive nephropathy in mice. Proceedings of the National Academy of Sciences. 2004; 101(23): 8687–8692. doi: 10.1073/pnas.0400035101
43. Lei XF, Fu W, Kim-Kaneyama J ri, et al. Hic-5 deficiency attenuates the activation of hepatic stellate cells and liver fibrosis through upregulation of Smad7 in mice. Journal of Hepatology. 2016; 64(1): 110–117. doi: 10.1016/j.jhep.2015.08.026